Structures 18 (2019) 128–137

Contents lists available at ScienceDirect

Structures

journal homepage: www.elsevier.com/locate/structures

Design of Truss Structures Through Reuse

Jan Brütting[a,*], Joseph Desruelle[a], Gennaro Senatore[b], Corentin Fivet[a]

[a] Structural Xploration Lab, Swiss Federal Institute of Technology (EPFL), Passage du Cardinal 13b, 1700 Fribourg, Switzerland
[b] Applied Computing and Mechanics Laboratory, Swiss Federal Institute of Technology (EPFL), Station 18, 1015 Lausanne, Switzerland

ARTICLE INFO

Keywords:
Structural optimization
Truss structures
Circular economy
Reuse
Life-Cycle Assessment

ABSTRACT

This paper presents structural optimization techniques to design truss structures that make best use of a given stock of structural components. Still little explored, the *reuse* of structural components over multiple service lives has the potential to significantly reduce the environmental impact of building structures. Structural design and construction based on reuse avoids sourcing new material, it reduces superfluous waste, and requires little energy. However, designing a structure from a stock of reclaimed elements entails a change of design paradigm: in contrast to conventional design practice, the structural geometry and topology depends on element stock characteristics, e.g. available cross sections and lengths. This paper presents discrete structural optimization formulations to design truss systems from stock elements. The approach taken in this work is iterative: 1) element assignment and topology optimization are carried out, and 2) geometry optimization follows thereafter to best-fit the system geometry to the length of assigned stock elements, for instance to reduce cut-off waste. Two case studies are presented: a) a cantilever of simple layout used to explain the details of the design methodology, and b) a train station roof structure of complex layout made from elements reused from disassembled electric pylons. For these case studies, Life Cycle Assessment confirms that an up to 63% environmental impact reduction is possible when comparing structures obtained with the proposed method against weight-optimized solutions made of new elements.

1. Introduction

1.1. Reuse and circular economy

The building sector is a major contributor to material consumption [1], energy use, greenhouse gas emission [2], and waste production [3]. Most of the *embodied impacts* of buildings [4], e.g. related to material extraction, production, construction and demolition, are due to load bearing systems [5]. A way to reduce these building embodied impacts is to apply the principles of *circular economy* [6]. In a circular economy, manufactured goods are kept in use as long as possible through closed loops, which consist of: 1) repair, 2) reuse, and 3) recycling.

Recycling is the common strategy to make use of obsolete construction materials but it involves energy for reprocessing (e.g. melting steel scrap). Instead, *reuse* has the potential to reduce building environmental impacts further with respect to recycling because less energy is spent for reprocessing [2,7]. This paper focuses on the direct reuse of structural components, involving their relocation and repurpose. In this context, reused structural elements will have a longer service life and disassembled buildings become a *mine* for new constructions [7]. A holistic approach to component reuse involves careful deconstruction as well as the storage, refurbishment and quality assessment of structural elements [7,8].

A recently built example of such design philosophy based on reuse is the BedZED project - a residential and office building whose steel structure is made of 90% locally reclaimed elements [9]. Another example is the London Olympic stadium roof truss that incorporates 2500 tons of reused steel pipeline tubes which were tested prior to reuse in order to assess the material quality [2]. A theoretical case study to design a railway station roof made of truss modules reclaimed from deconstructed industrial buildings and combined with new steel elements is presented in [10]. The reuse of such truss modules allowed saving 30% of embodied energy and carbon compared to a new steel structure [10].

Even though significant environmental savings are possible through reuse [7], it has been shown that reusing steel elements can be more expensive in monetary terms than using new steel because of the deconstruction and refurbishment processes involved [11,12]. It was identified in [7] and [12] that the potential establishment of element stocks, databases and a market for reused elements will facilitate greater reuse in the future.

* Corresponding author at: Structural Xploration Lab, IA ENAC EPFL, smart living lab, Passage du Cardinal 13b, 1700 Fribourg, Switzerland.
E-mail address: jan.bruetting@epfl.ch (J. Brütting).

https://doi.org/10.1016/j.istruc.2018.11.006
Received 14 September 2018; Received in revised form 6 November 2018; Accepted 7 November 2018
Available online 10 November 2018

Notation

Variable	Unit	Description
$a \in \mathbb{R}^s$	[m^2]	vector of stock element cross section areas
$B \in \mathbb{R}^{d \times m}$	[−]	equilibrium matrix
b	[m]	buffer on the available element length
C	[$kgCO_2eq$]	total embodied carbon
$D \in \mathbb{R}^{d \times m}$	[m]	matrix to account for self-weight of the structure
d	[−]	number of unsupported degrees of freedom
E	[MJ]	total embodied energy
$e \in \mathbb{R}^s$	[MPa]	vector of stock element Young's moduli
$f \in \mathbb{R}^d$	[MN]	vector of static external forces
i	[−]	truss member position i
j	[−]	stock element group j
k	[−]	kth load case
$l \in \mathbb{R}^s$	[m]	vector of stock element lengths
$\bar{l} \in \mathbb{R}^m$	[m]	vector of truss member lengths
m	[−]	total number of truss member positions
$n \in \mathbb{R}^s$	[−]	vector of stock element availabilities
$p \in \mathbb{R}^m$	[MN]	vector of truss member forces
$p_{i,\,j}^{\,buck.}$	[MN]	buckling resistance of element j assigned at truss position i
$\rho \in \mathbb{R}^s$	[kg/m^3]	vector of stock element densities
s	[−]	total number of stock element groups
$\sigma \in \mathbb{R}^s$	[MPa]	vector of stock element yield strengths
$T \in \{0,1\}^{m \times s}$	[−]	binary assignment matrix
$u \in \mathbb{R}^d$	[m]	vector of nodal displacements
$u_{min} \in \mathbb{R}^d$	[m]	lower bound on the nodal displacement
$u_{max} \in \mathbb{R}^d$	[m]	upper bound on the nodal displacements
$x \in \mathbb{R}^d$	[m]	vector of coordinates for unsupported truss nodes
$y \in \mathbb{R}^s$	[MN/m^3]	vector of stock element specific weights

1.2. Structural design

Reuse involves reversing the conventional structural design process, because the synthesis of a structural layout (geometry and topology) is constrained by mechanical and geometric properties of an available stock of elements [13]. This paper presents applications of structural optimization methods previously developed by the authors [14] to design structures through reuse.

Optimization is often employed to obtain optimal layouts of structures under a given set of boundary conditions and constraints [15]. Truss structures are usually optimized by adjusting the topology starting from a *ground structure* [16], which is the set of all possible member positions between the truss nodes. The member cross section sizes are part of the design variables. Simultaneously [17] or sequentially [18], the node positions can also be changed in order to obtain an optimal truss geometry. To reduce optimization complexity, often cross section areas are treated as continuous variables. In practice, because only a limited set of standard cross sections is available, discrete sizing optimization should be employed [19]. Discrete sizing and topology optimization has been formulated as a Mixed-Integer Linear Programming (MILP) problem in [20] and [21]. A MILP problem can be solved to global optimality employing combinatorial optimization techniques such as *branch-and-cut* methods [22]. Usually, optimization of truss structures is carried out assuming that all elements can be fabricated with required cross sections and lengths. Conversely, when reusing structural elements from a stock, the number of available cross section types is restricted and the structure geometry has to best-fit available element lengths.

Structural optimization with stock constraints has received little attention so far. The optimization of plane frames of fixed topology from a stock of onetime available cross sections is presented in [23], where evolutionary algorithms have been employed for weight optimization but without accounting for available element lengths. Strategies based on algorithms developed to solve bin-packing problems have been employed to form-fit a stock of wood logs to statically determinate trusses in [24].

1.3. Outline

Section 2 summarizes an optimization approach for reticulated structures subject to a constraining element stock. This approach combines 1) discrete structural topology optimization methods to select an optimal subset of stock elements (Sections 2.1 and 2.2), with 2) geometry optimization methods to optimally match structure geometry and stock element dimensions (Section 2.3). Section 2.4 introduces an extension to this method to obtain improved solutions. Section 3 presents the main assumptions of a Life Cycle Assessment that is employed to quantify environmental impacts and savings through reuse. Section 4 describes two case studies: a) a cantilever truss of simple layout to explain in detail the design methodology (Section 4.1), and b) a train station roof structure of complex layout reusing elements from a realistic set of disassembled electric pylons (Section 4.2).

2. Structural optimization with stock constraints

2.1. Element assignment

The selection of suitable elements from a stock and their optimal placement in a structure can be formulated as an assignment problem which is of combinatorial nature. This is comparable to the selection of cross sections in discrete sizing optimization methods [20,21]. Fig. 1(a) shows a weight optimized cantilever truss obtained from the ground structure shown by the dashed lines ($m = 5$ potential bar positions) and using the stock illustrated in Fig. 1(c). The stock comprises $s = 6$ element groups which are characterized by material properties (i.e. Young's moduli $\boldsymbol{e} \in \mathbb{R}^s$, material strengths $\boldsymbol{\sigma} \in \mathbb{R}^s$, material densities $\rho \in \mathbb{R}^s$, specific weights $\boldsymbol{y} \in \mathbb{R}^s$), cross-section areas $\boldsymbol{a} \in \mathbb{R}^s$, element lengths $\boldsymbol{l} \in \mathbb{R}^s$ and the element availabilities $\boldsymbol{n} \in \mathbb{R}^s$.

The assignment of one element from stock group j at position i in the structure, is represented by an entry $t_{i,j} = 1$ in the binary assignment matrix $\boldsymbol{T} \in \{0, 1\}^{m \times s}$, shown in Fig. 1(b). For clarity, the system topology is changed when no element is assigned at a certain position, corresponding to a row of zeros in the assignment matrix. The inequalities (Eqs. (1) and (2)) ensure maximally one assignment per position i and limit the selection of bars to the number of available elements for each group j:

$$\sum_{j=1}^{s} t_{i,j} \leq 1 \quad \forall\, i = 1...m \tag{1}$$

$$\sum_{i=1}^{m} t_{i,j} \leq n_j \quad \forall\, j = 1...s \tag{2}$$

$$t_{i,j} \in \{0, 1\} \quad \forall\, i, j$$

2.2. Structural assignment and topology optimization problem

The assignment problem described in Section 2.1 is included into a structural optimization formulation using a Simultaneous ANalysis and Design (SAND) [25] approach. Different to Nested ANalysis and Design (NAND) where design sensitivity analysis is performed at each iteration of the optimization, SAND formulations simultaneously treat design variables (e.g. cross section areas) as well as state variables (e.g. internal forces and nodal displacements) as variables of the mathematical programming procedure [25,26]. The SAND approach is key to allow

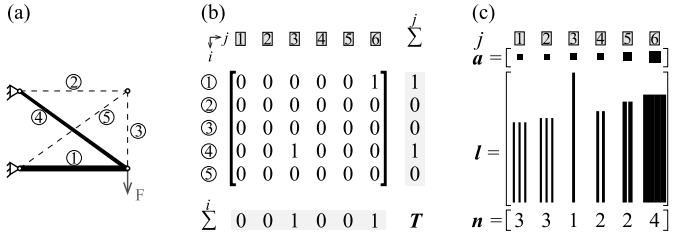

Fig. 1. Assignment of stock elements: (a) ground structure, (b) assignment matrix, (c) stock.

formulating discrete assignment and topology optimization as a MILP problem and to solve it to global optimality [21,26]. The objective of the optimization is to reduce the structural mass M and consequently to maximize element capacity utilization. The problem of assignment and topology optimization from a stock of reused elements is formulated as:

(P)

$$\min_{\boldsymbol{T},\boldsymbol{p},\boldsymbol{u}} M(\boldsymbol{T}) = \bar{\boldsymbol{l}}^T \boldsymbol{T}(\boldsymbol{a}\circ\boldsymbol{\rho}) \tag{3}$$

$$\boldsymbol{B}\boldsymbol{p}^{(k)} = \boldsymbol{f}^{(k)} + \boldsymbol{D}\boldsymbol{T}(\boldsymbol{a}\circ\boldsymbol{y}) \quad \forall\, k \tag{4}$$

$$\boldsymbol{b}_i^T \boldsymbol{u}^{(k)} \sum_{j=1}^{s} \frac{e_j a_j}{\bar{l}_i} t_{i,j} = p_i^{(k)} \quad \forall\, i,\, k \tag{5}$$

$$-\boldsymbol{T}(\boldsymbol{a}\circ\boldsymbol{\sigma}) \le \boldsymbol{p}^{(k)} \le +\boldsymbol{T}(\boldsymbol{a}\circ\boldsymbol{\sigma}) \quad \forall\, k \tag{6}$$

$$-\sum_{j=1}^{s} t_{i,j} p_{i,j}^{buck.} \le p_i^{(k)} \quad \forall\, i,\, k \tag{7}$$

$$\boldsymbol{u}_{min}^{(k)} \le \boldsymbol{u}^{(k)} \le \boldsymbol{u}_{max}^{(k)} \quad \forall\, k \tag{8}$$

$$\bar{l}_i \sum_{j=1}^{s} t_{i,j} \le \sum_{j=1}^{s} t_{i,j} l_j \quad \forall\, i = 1...m \tag{9}$$

Formulation (P) includes the design variables of the assignment matrix $\boldsymbol{T}$ as well as the state variables of member forces $\boldsymbol{p}^{(k)} \in \mathbb{R}^m$ and nodal displacements $\boldsymbol{u}^{(k)} \in \mathbb{R}^d$. The vector $\boldsymbol{u}^{(k)}$ has size d which is the number of free degrees of freedom. The structural mass (Eq. (3)) is computed as the inner product of truss member lengths $\bar{\boldsymbol{l}} \in \mathbb{R}^m$, element cross section areas $\boldsymbol{a}$ and material densities ρ assigned through $\boldsymbol{T}$. The operator ∘ indicates an element-wise multiplication of vector entries (Hadamard product). For each load case k, static equilibrium of forces at the nodes is ensured by Eq. (4), where $\boldsymbol{B} \in \mathbb{R}^{d\times m}$ is the equilibrium matrix and $\boldsymbol{f}^{(k)} \in \mathbb{R}^d$ is the vector of static external forces. Self-weight is added to the external force vector through the product of the matrix $\boldsymbol{D} \in \mathbb{R}^{d\times m}$ and the assigned element cross section areas $\boldsymbol{a}$ and specific weights $\boldsymbol{y}$. The matrix $\boldsymbol{D}$ holds entries of half the member lengths $\bar{l}_i$ at corresponding vertical degrees of freedom at the member ends.

Geometric compatibility constraints in Eq. (5) relate element elongation, nodal displacements and member force. Member forces are bounded by the admissible stress $\boldsymbol{\sigma}$ in tension and compression (Eq. (6)). In addition, local member buckling is considered via Eq. (7), where $p_{i,\,j}^{\,buck.}$ represents the buckling resistance of stock element j at position i in the truss. The numeric value of the buckling resistance can be calculated from the Euler buckling formulation or according to code regulations [27]. Nodal displacements are bounded by serviceability limits (Eq. (8)). Eq. (9) constrains the stock assignment to elements that are longer or equal to the structure's member lengths $\bar{\boldsymbol{l}}$. To complete the optimization formulation, the assignment and availability constraints introduced in previous Section 2.1 must hold (Eqs. (1) and (2)).

The objective function and all constraints of (P) are linear, except the compatibility constraints (Eq. (5)) which contain products of binary assignment variables $t_{i,j}$ and continuous displacement variables $\boldsymbol{u}$. As shown in [21], these "bi-linear" constraints can be reformulated into linear constraints by "big-M" techniques and the introduction of auxiliary continuous variables. Consequently, (P) is equivalently described as a MILP problem, which can be solved to global optimality. This formulation draws from work presented in [21], yet differs in the way that it includes self-weight and buckling (Eqs. (4) and (7)) as well as the constraints on availability and element lengths (Eqs. (2) and (9)).

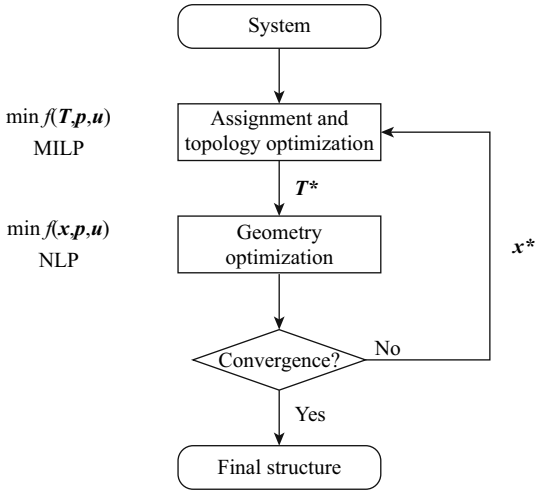

Fig. 2. Iterative layout optimization process.

2.3. Layout optimization

The assignment and topology optimization method of Section 2.2 is combined with geometry optimization to formulate a general structural layout optimization method. Fig. 2 shows a flow chart describing this sequential approach. First, given a fixed geometry, problem (P) is solved to global optimality resulting in an optimal assignment and topology $\boldsymbol{T}^*$. In this step, the length of an assigned element may not match exactly the distance between the nodes of the corresponding ground structure position. Geometry optimization is then carried out by varying the positions $\boldsymbol{x} \in \mathbb{R}^d$ of all free nodes to match the assigned element lengths. The geometry optimization step is formulated as a general Non-Linear Programming (NLP) problem and solved to local optimality. The reader is referred to [14] for a detailed explanation of the geometry optimization step involving stock constraints. Convergence of the layout optimization is reached when no further mass and waste reductions are achieved in successive iterations.

2.4. Element buffer

Starting from the ground structure (step 1), it might not be possible to assign all the required stock elements because they might be too short for certain positions. However, because of the iterative geometry optimization, successive nodal position changes might allow their assignment in later steps. As an extension to the method given in [14], this paper introduces an absolute *buffer b* on the element length to allow infeasible length assignments at the start of the iterative search. Constraint (Eq. (9)) becomes:

$$\bar{l}_i \sum_{j=1}^{s} t_{i,j} \le \sum_{j=1}^{s} t_{i,j}(l_j + b) \quad \forall\, i = 1...m \tag{10}$$

This buffer reduces to zero within a fixed number of iterations. In other words, the search space is temporarily increased to allow more assignment combinations at the start of the sequential optimization. However, element length constraints (Eq. (9)) are satisfied for the final result.

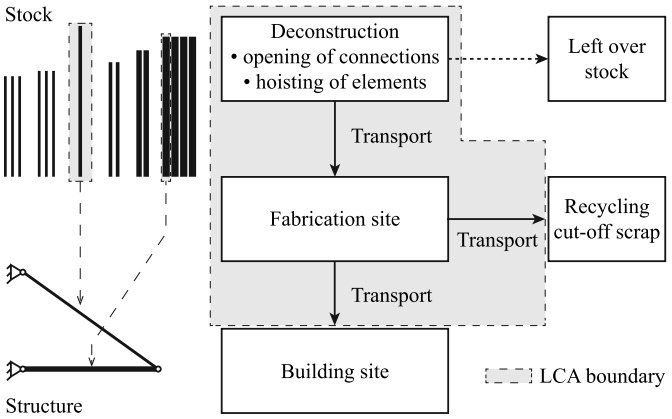

Fig. 3. Sub-processes and boundary of the Life Cycle Assessment for the case of reusing structural elements.

3. Embodied energy and carbon

The aim of reusing structural elements is the reduction of environmental impacts. Life Cycle Assessment (LCA) is carried out to quantify the embodied energy and carbon of steel structures obtained using the method described in Section 2. This way, the environmental impacts of structures made from reused elements are compared to those of structures comprising new elements made of recycled steel. In this assessment, only the impacts of processes that differ between reuse and recycling scenarios are considered. The study period begins with the processes required to supply structural elements and ends when the structure is transported to the building site. Fig. 3 shows the boundary and the processes that are included in the assessment of reusing steel elements, which involves evaluating the impacts of: 1) selective deconstruction of obsolete buildings (opening connections, hoisting elements with a crane), and 2) the transport of elements from deconstruction site to building site.

Environmental impacts of selective deconstruction are mostly caused from the use of machines during disassembly. In this paper, the calculation of these impacts is based on data reported in [28] that considers the deconstruction of office building steel structures via a mobile crane and via worker crews equipped with pneumatic ratchets powered by compressors.

Impacts related to refurbishment, reshaping or storing of elements are neglected because they are assumed small. Any impacts related to manufacturing connections are neglected because it is assumed that such impacts are small and of similar intensity in both scenarios (reuse and recycling). Further, it is assumed that leftover stock elements can be used elsewhere, thus only the elements assigned to the final structure contribute to the environmental impacts.

The impacts caused by transporting the selected stock elements as well as the final structure are computed via datasets given in the German Life Cycle Inventory *Ökobaudat* (open-access, available in English) [29]. For the reuse and the recycling case total transport distances of 200 km and 70 km are considered respectively.

Table 1
Characterization - stock A and B.

Stock A				Stock B			
CHS type	a_j [cm^2]	l_j [m]	n_j [–]	CHS type	a_j [cm^2]	l_j [m]	n_j [–]
21.3 × 3.2	1.82	1.25	3	21.3 × 3.2	1.82	1.80	1
33.7 × 3.2	3.07	2.50	3	21.3 × 3.2	1.82	2.60	3
33.7 × 4.0	3.73	3.25	2	33.7 × 4.0	3.73	2.50	2
42.4 × 4.0	4.83	2.50	2	42.4 × 4.0	4.83	1.50	2
42.4 × 5.0	5.87	3.25	3	48.3 × 5.0	6.80	2.50	2
48.3 × 5.0	6.80	3.00	1	48.3 × 5.0	6.80	1.80	2

The total embodied energy E and embodied carbon C of structures made from reused elements can be expressed as a function of the structural mass M as well as the cut-off waste ΔM:

$$E_{Reuse} = 3.245\frac{\text{MJ}}{\text{kg}}M + 3.235\frac{\text{MJ}}{\text{kg}}\Delta M \tag{11}$$

$$C_{Reuse} = 0.277\frac{\text{kgCO}_2\text{eq}}{\text{kg}}M + 0.276\frac{\text{kgCO}_2\text{eq}}{\text{kg}}\Delta M \tag{12}$$

To benchmark the environmental savings obtained through reuse against newly produced elements, common production methods involving primary and secondary (recycled) steel are considered. The assessment of these impacts is based on environmental product declarations reported in *Ökobaudat* [29]. The total environmental impacts for conventionally produced new steel profiles and their transport to the site are:

$$E_{New} = 13.227\frac{\text{MJ}}{\text{kg}}M \tag{13}$$

$$C_{New} = 0.925\frac{\text{kgCO}_2\text{eq}}{\text{kg}}M \tag{14}$$

It is assumed that first-hand steel members are produced with exact lengths and do not generate impacts related to waste. For more details on the LCA assumptions and on Eqs. (11) to (14), the reader is referred to [14].

4. Case studies

4.1. Cantilever truss

4.1.1. System and stock

Fig. 4(a) shows a 10-bar cantilever ground structure with a span S of 4.00 m and a height of 2.00 m. A load F = 10 kN is applied at the bottom end. For the geometry optimization step the free nodes 2, 3, 5 and 6 are bounded within ± 0.80 m distance from their initial position (Fig. 4(a), grey domains). The horizontal position of node 3 is further constrained to maintain a minimum span of 4.00 m. Limiting node positions to defined domains prevents merging nodes and self-

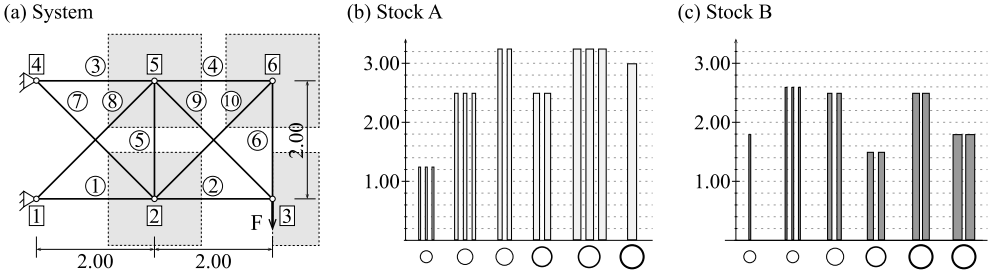

Fig. 4. (a) 10-bar cantilever ground structure, (b) stock A, (c) stock B.

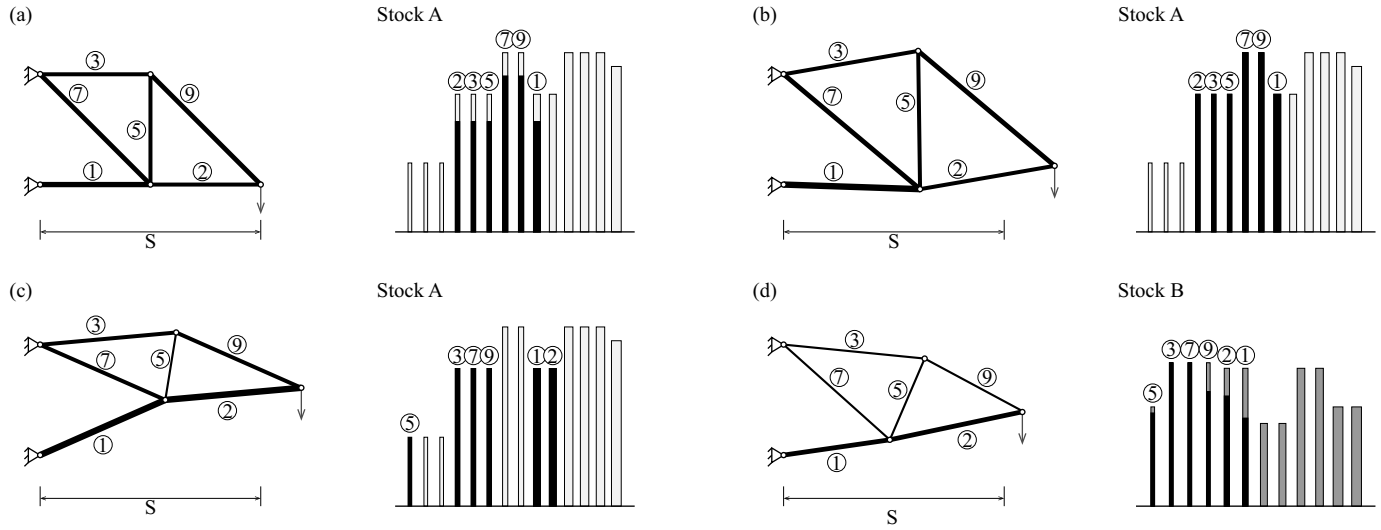

Fig. 5. Cantilever truss results: (a) pure assignment and topology optimization, (b) layout optimization without element buffer, (c) and (d) layout optimization with element buffer.

overlapping of the structure. In practice, the constraining domains also allow to obtain optimal structure geometries that remain close to an initial design intention or input.

Two stock configurations A and B are illustrated in Fig. 4(b) and (c). The two stocks consist of steel bars with circular hollow sections (CHS) of dimensions taken from EN 10220 [30]. It is assumed that all steel bars have a yield strength of 235 MPa, a Young's modulus of 210 GPa and a density of 7850 kg/m^3. Table 1 summarizes cross-section types and areas as well as element lengths and availabilities for each group in stocks A and B.

4.1.2. Results

Four cases for the optimization of the cantilever truss are considered: (a) pure assignment and topology optimization from stock A; (b) layout optimization without element buffer from stock A; (c) and (d) layout optimization with element buffer from stock A and B respectively. In addition to these cases with reused elements, two benchmark scenarios for weight-optimized structures made of newly produced steel elements with equivalent material properties are considered. These benchmark cases are: (e) a sequential discrete cross section and

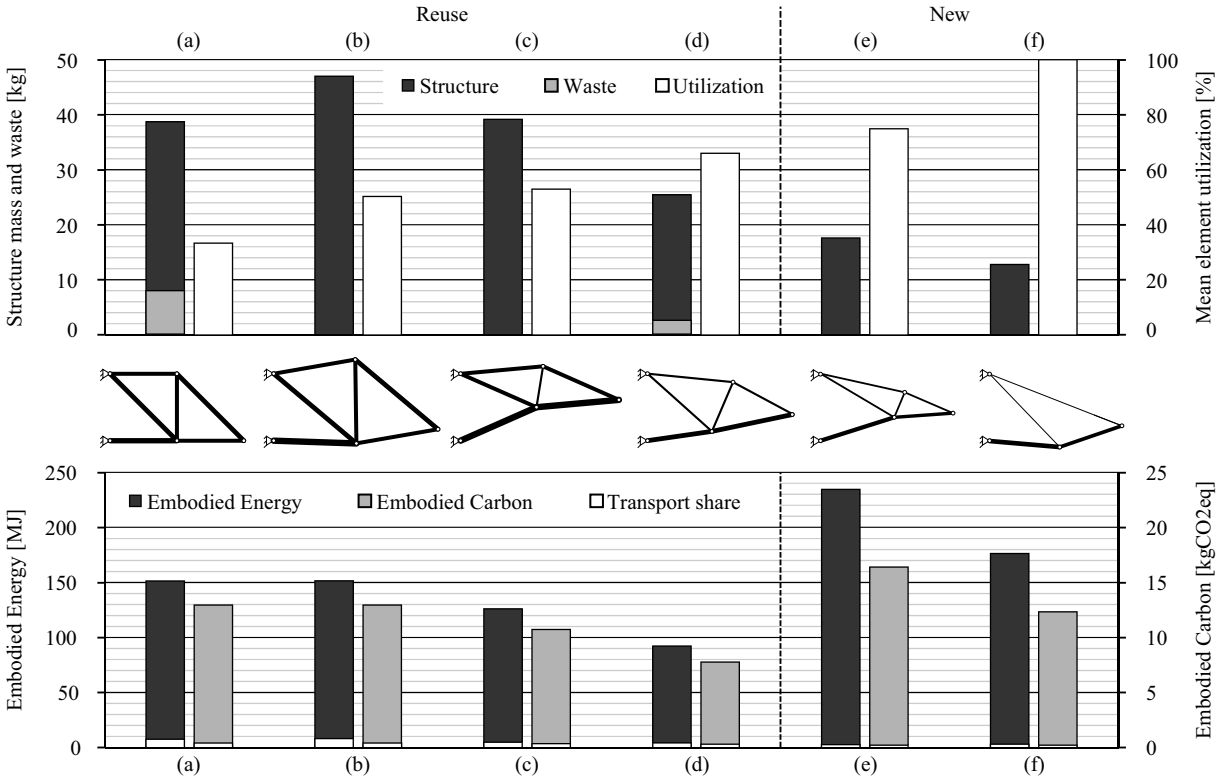

Fig. 6. Comparison between structures: (a) to (d) made from reused elements, (e) and (f) made of new steel.

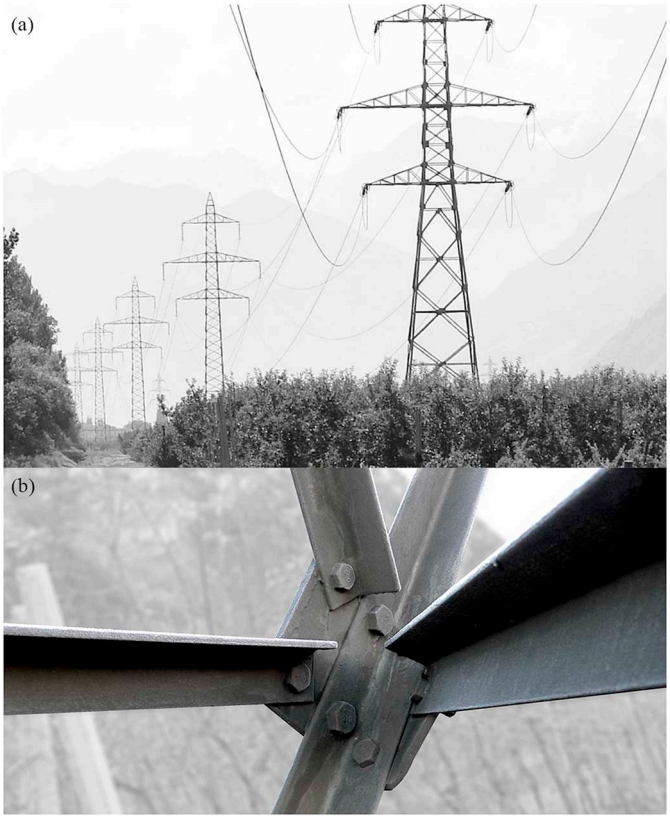

Fig. 7. (a) Power transmission line (Swissgrid AG, with permission), (b) typical sections and connection detail.

geometry optimization allowing all standard CHS sections reported in EN 10220 [30], and (f) a simultaneous cross section and geometry optimization in which cross section radii are continuous design variables and the wall thickness is set to 10% of the radius. In case (e), during the geometry optimization step compliance is minimized whereas during the sizing optimization step weight minimization is the objective. For case (f) the objective is weight minimization. All cases consider a critical Euler buckling capacity (Eq. (7)).

Fig. 5 shows the optimal structural systems as well as the use of the stock for the cases (a) – (d) involving reuse. In the stock illustrations, black bars represent system members and grey bars unused stock elements or cut-off. In addition, Fig. 6 shows obtained results for all cases, including (e) and (f). Case (a) results in the biggest cut-off waste ΔM of 8.00 kg, whereas cases (b) and (c) achieve zero waste because of geometry optimization. Case (d) achieves the lowest mass amongst all the structures made from reused elements because stock B has a larger availability of small sections than stock A. In cases (a) and (b), small cross sections cannot be used because of their short length. In case (c), the assignment of a small cross section at position ⑤ is possible via the element buffer technique described in Section 2.4. The element buffer also allows obtaining an optimal solution in case (d) where all stock elements are shorter than the initial ground structure diagonals.

The bar chart at the top of Fig. 6 further indicates the mean capacity utilization of all truss members. Obviously, using lighter stock elements results in an increased utilization – for example compare cases (b) and (c). As stock B contains elements with smaller cross sections than stock A, the capacity utilization in case (d) is even higher than in case (c). In benchmark case (e) all cross sections reported in EN 10220 [30] are available in infinite quantity, allowing for a lighter structural system. Nevertheless, the discrete nature of the sizing problem results in a maximum utilization of 75%. Only the members in benchmark case (f), in which the cross section areas are treated as continuous variables, reach full capacity utilization and by that achieve the lightest structure. In general, member capacity utilization indicates that reusing structural elements can result in oversized structures when there is a limited availability of small cross sections.

4.1.3. Embodied impact savings

The embodied energy and carbon of the systems made from reused elements are compared to those of weight-optimized structures made from newly produced elements following the method introduced in Section 3. The bar chart at the bottom of Fig. 6 shows that reusing structural elements results in a significant reduction of embodied carbon and energy, even though these systems have a higher mass and lower mean capacity utilization. The environmental impacts due to the transportation of elements are small compared to the remaining shares caused by selective deconstruction for the reuse cases (a) to (d) or by new production for the benchmark cases (e) and (f).

4.2. A train station roof designed from power transmission pylons

This case study proposes a structural scheme for the main train station roof in Lausanne (Vaud, Switzerland) using elements reclaimed from power transmission pylons. The redesign of Lausanne's train

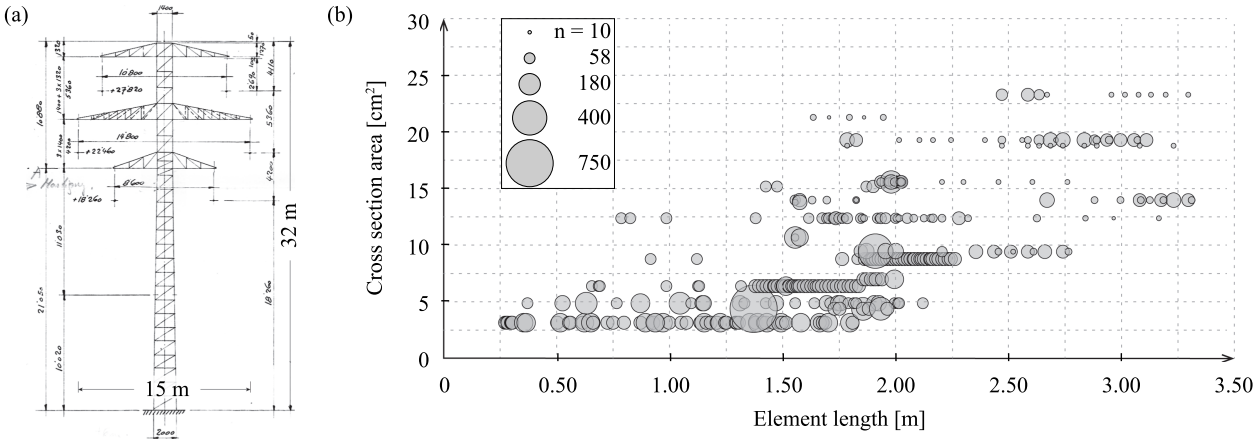

Fig. 8. (a) Original drawing of one pylon section (Swissgrid AG, with permission), (b) stock composition.

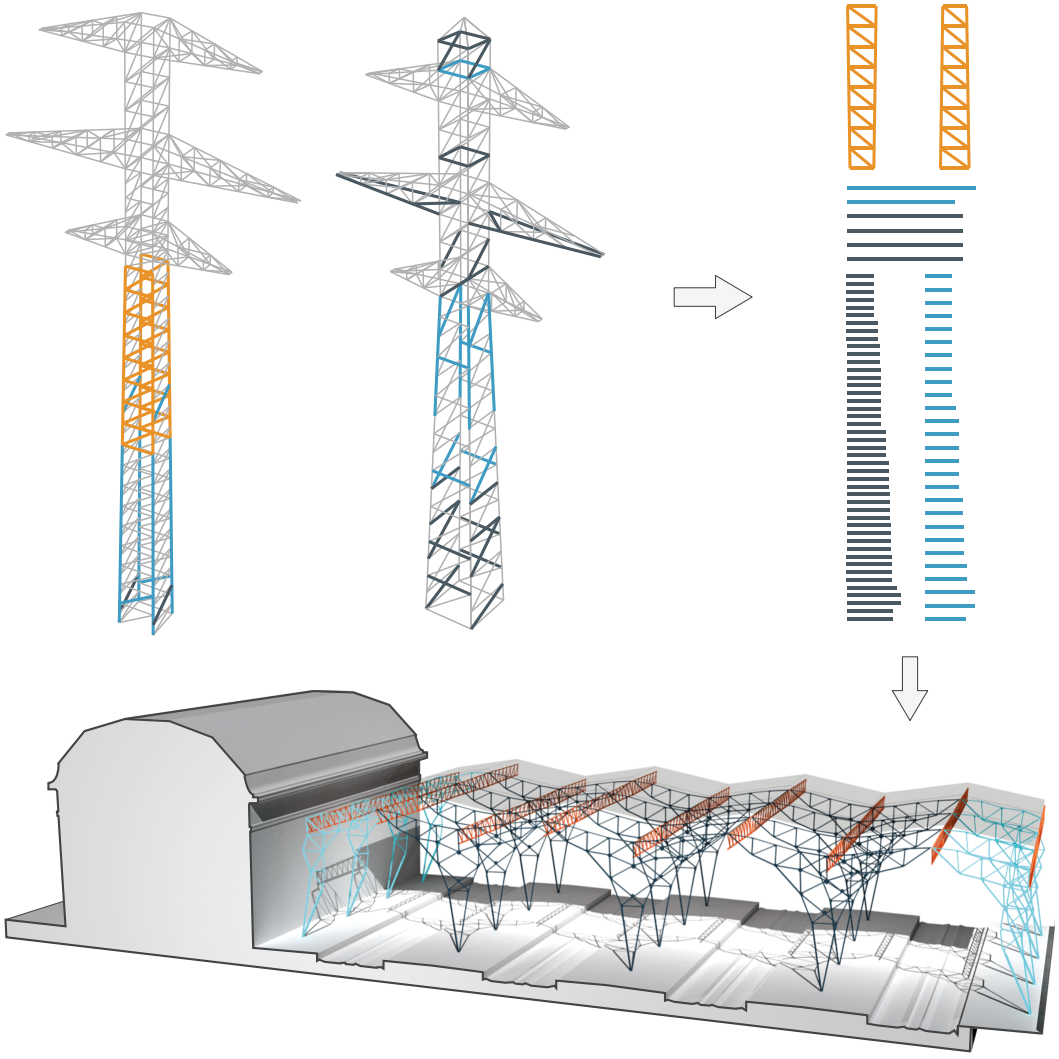

Fig. 9. Schematic view of the intended roof truss design, using elements from electric pylons. (For interpretation of the references to color in this figure, the reader is referred to the web version of this article.)

station is currently under planning to respond to an increase in passenger demand. The pylons, shown in Fig. 7(a), were built in the 1950s in the region of Wallis, Switzerland. Six power transmission lines consisting of such pylons are scheduled to be replaced by one high voltage line. However, the pylon members have not yet reached the service life for which they had been designed.

4.2.1. Stock characterization

The pylons consist of L-section steel bars connected by plates and bolts as shown in Fig. 7(b). The power line operator *Swissgrid* AG intends to disassemble the pylons piece by piece. Fig. 8(a) shows one of the archive plans that have been used to quantify the number of elements within one transmission line as well as their mechanical

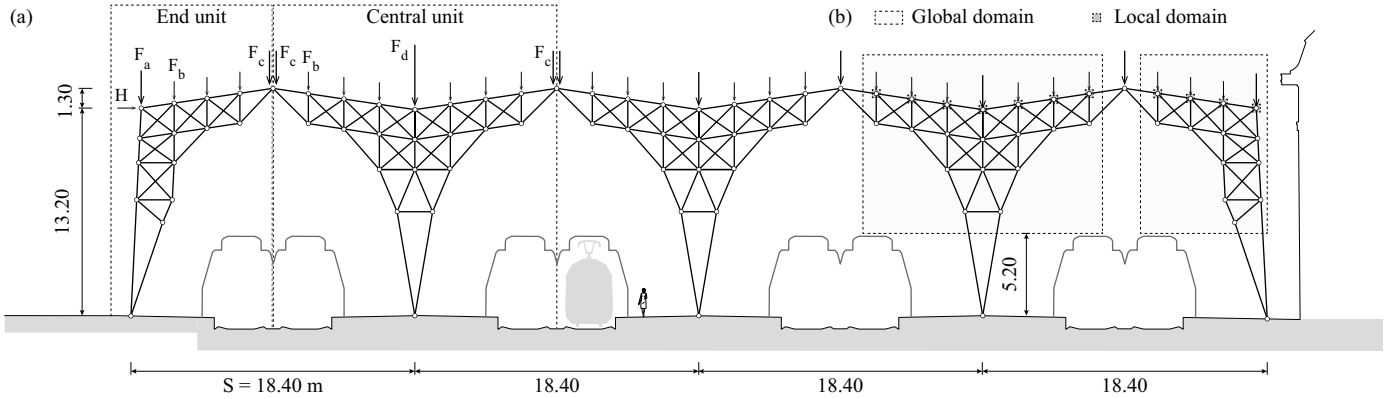

Fig. 10. Transversal section: (a) ground structure and loads, (b) geometry optimization domains.

properties, cross section areas, connection detailing and lengths. One single line comprises about 50 pylons, totaling up to 19,000 bars. Fig. 8(b) shows a scatter diagram of 332 different bar groups. In addition, some longer and stronger elements taken from the pylon corners are available. For most elements the plans report a "historic" steel grade of St37 that is comparable to grade S235 steel commonly used today. To quantify the element axial force capacities, not only stress limits (Eq. (6)) but also a reduced tension capacity due to existing hole patterns are taken into account. In addition, critical buckling loads (Eq. (7)) of the L-sections are computed in accordance with Swiss standard SIA 263 [31].

4.2.2. Roof structure design

Fig. 9 presents a schematic view of the intended roof design, whose primary transversal section comprises three central units (black) and two end units (blue). The primary structure spans over four double-tracks as an array of three-hinged frame trusses and is repeated 21 times. This way the roof structure covers an area of 200 m × 75 m. Parallel to the tracks, secondary trusses (Fig. 9, orange) span 10 m between multiple transverse sections. The secondary trusses are taken from the electric pylons as complete modules similar to the approach shown in [10]. Reusing complete modules can reduce labor by avoiding element-by-element disassembly. However, for the primary system, more design freedom is sought and therefore the optimization method of Section 2 is employed.

Fig. 10(a) shows the ground structure of end and central units. The ground structure layout is predetermined to meet site constraints, such as support locations and required heights. Further, the spacing of the ground structure nodes is chosen to be similar to the length distribution of available elements. In the geometry optimization step, the free nodes are globally bounded by the domains shown in grey in Fig. 10(b). In addition, the admissible horizontal and vertical shifts of the top chord nodes are constrained to ± 50 cm from their original position in order to achieve a regular distribution in the optimized layout.

The load cases and limit states considered in the optimization are reported in Table 2. The self-weight of the structure, a superimposed dead load caused by a roof cover as well as snow and wind actions are taken into account. Two load combinations are considered (Table 2): one for ultimate limited state (ULS) and one for serviceability limit state (SLS). Through a preliminary design, the selected ULS combination of actions was identified as the governing one and therefore used in the optimization. Because the roof is not accessible nor connected to any other non-structural element, only quasi-permanent loading is considered for the serviceability limit state, where deflections are limited to $S/300 = 61.3$ mm. These assumptions on loading and limit states are made in accordance to the Swiss standards SIA 260 [32] and 261 [33].

The distributed loads reported in Table 2 are converted into corresponding nodal loads applied to the primary structure. The location of the applied loads is shown in Fig. 10(a) for both, end and central unit. Table 3 gives the corresponding load magnitudes.

The optimization procedure outlined in Section 2, is employed to optimize end and central units separately, which reduces computational cost. Even though both units are treated individually, any horizontal reactions transmitted from the end to the central unit are taken into account. From the 332 pylon element groups two subsets of 71 and 91 stock elements were selected for the end and central unit respectively. This selection considers the element availability to allow the design of the complete roof structure (20 bays). The selection is further narrowed to exclude elements of very small length. As a result, the number of possible assignments is decreased and the computational complexity is further reduced.

In this case study elements are intended to be joined at nodes with custom connection plates in order to reuse elements at their full length and existing bolt holes. This reduces labor to unbolting and reassembly and it potentially avoids any element cutting. In addition, the possibility of using custom connection plates can compensate small gaps when a distance between nodes is bigger than the assigned stock element length. Consequently, during the geometry optimization step the nodal positions are adjusted such that the distance between nodes are greater than the assigned element lengths. In addition, in the assignment and topology optimization step the inequality sign of Eq. (10) is reversed and the buffer is a negative number.

Table 2
Assumed load cases, limit states and displacement limits.

Load case	Description	Load magnitude
g_0	Self-weight	From assignment
g_1	Dead load	0.50 kN/m^2
q_s	Snow load	1.00 kN/m^2
q_w	Wind load	1.30 kN/m^2
Limit state		
ULS	$1.35(g_0 + g_1) + 1.5q_s + 0.6q_w$	
SLS	$1.00(g_0 + g_1)$	
Displacement limits		
SLS	$S/300 = 18{,}400/300 = 61.3$ mm	

Table 3
Nodal vertical and horizontal loads considered in the optimization.

Load combination	H [kN]	F_a [kN]	F_b [kN]	F_c [kN]	F_d [kN]
ULS	11	86	16	79	158
SLS	0	26	4	22	44

4.2.3. Results

Fig. 11 shows the initial ground structure (dashed lines) and the obtained layout (black) of the final transversal roof section. Topology optimization successfully reduces the number of truss diagonals to

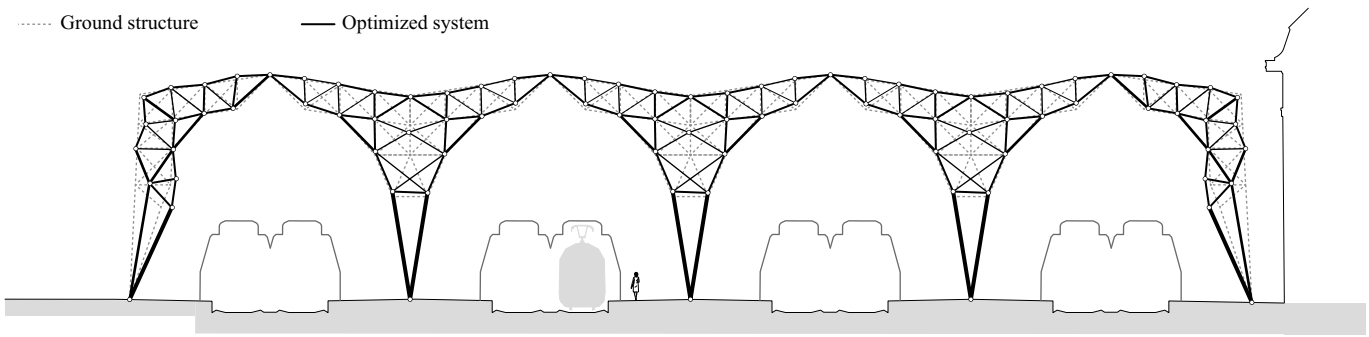

Fig. 11. Optimal transversal section layout.

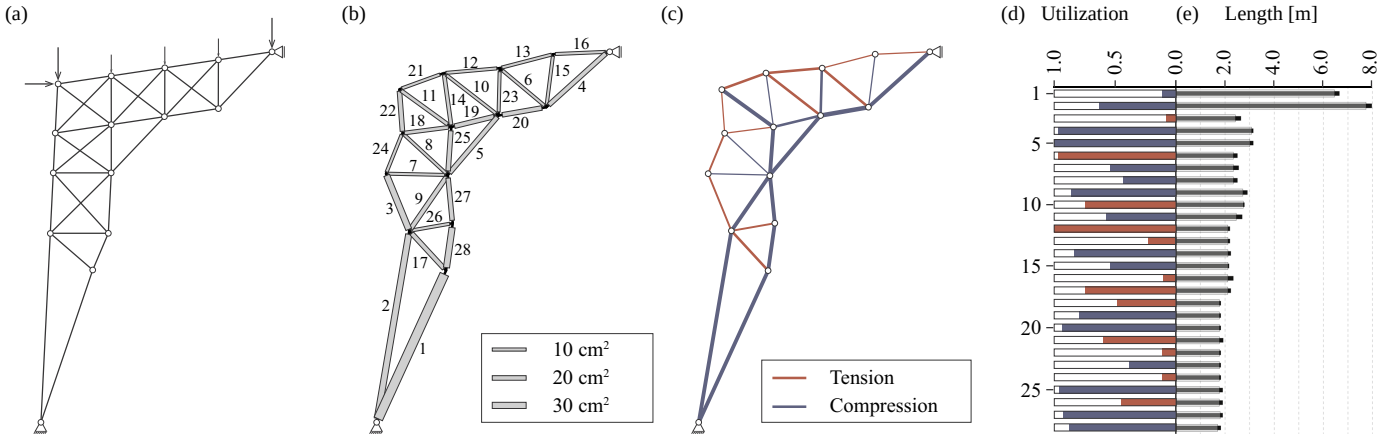

Fig. 12. End unit: (a) ground structure, (b) final layout, (c) internal force distribution (d) capacity utilization, (e) stock use, element lengths (grey bars) and distance between nodes (black bars).

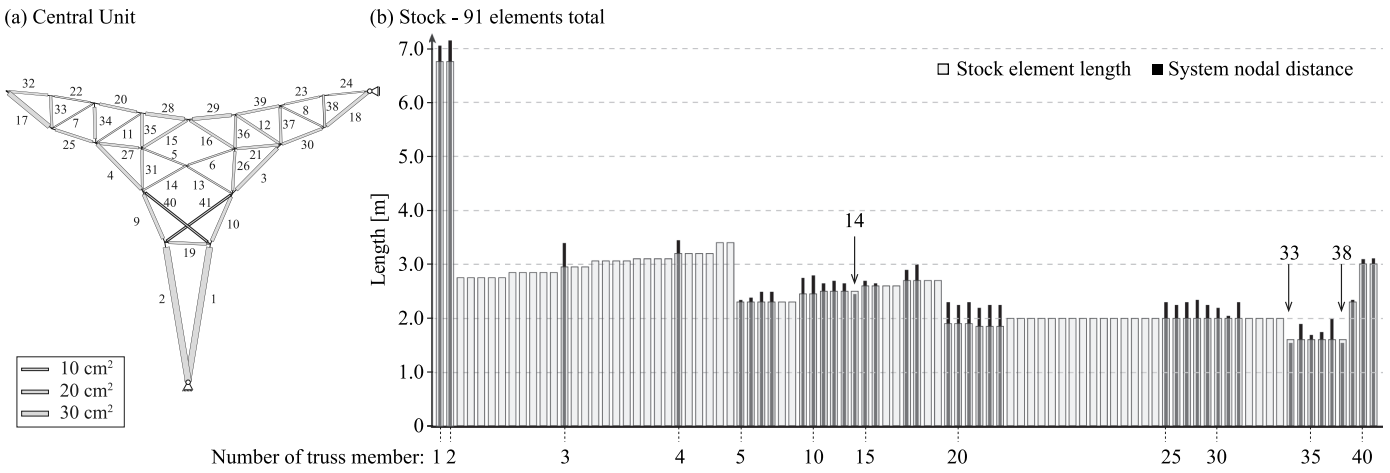

Fig. 13. Central unit: (a) final layout and cross section areas, (b) stock use, element lengths (grey bars) and distance between nodes (black bars).

Table 4
Environmental impacts of (a) the benchmark case (b) the reuse case.

Metric	Unit	(a) New elements	(b) Reused elements	(b) vs. (a)
Mass	[kg]	4,400	6,600	+50%
Mean cross section area	[cm^2]	9.8	12.00	+22%
Mean element utilization	[%]	84%	62%	−22% (abs)
Embodied energy	[MJ]	58,200	21,400	−63%
Embodied carbon	[$kgCO_2eq$]	4,100	1,800	−56%

reduce weight.

Fig. 12 shows (a) the ground structure used for the optimization of the end units and (b) the optimal layout and assignment labeling. Fig. 12(c) maps the internal forces onto the structure geometry - the line thickness is proportional to the force magnitude. Fig. 12(d) shows the capacity utilization of each assigned stock element considering tension, compression and buckling. Fig. 12(e) illustrates the used stock elements (grey bars) and the corresponding distance between nodes (black bars). For all bar positions, the distance between connected nodes is bigger than the assigned stock element length.

Fig. 13(a) shows the obtained layout and cross section areas of the central unit. The labels in Fig. 13(a) relate truss members to assigned stock elements in Fig. 13(b). In Fig. 13(b) grey bars indicate the stock element lengths whereas black overlays on each assigned stock element represent the corresponding nodal distance in the truss. In total, 41 out of the 91 stock members are used in the truss. The geometry optimization has maximized the number of stock elements that can be used at their full length with existing holes. However, no large enough nodal distance could be found for members 14, 33 and 38 (Fig. 13(b)). A detailed connection design would be required to evaluate whether all elements could be joined without cutting and whether there is no overlap of cross section profiles. Such study goes beyond the scope of this paper.

Because the optimization only considered two limit states, the complete three-dimensional roof structure (20 bays) has been analyzed by means of Finite Element Analysis taking into account additional load cases. The final design is marginally different to that obtained by the optimization, requiring only minor changes in topology and local reinforcement - as for instance the introduction of the two cross bracing members 40 and 41 shown in Fig. 13(a).

4.2.4. Environmental impact comparison

The environmental impacts of the structure made from reused elements are compared to those of a structure with identical layout (topology and geometry) optimized for minimum weight whilst allowing all discrete L-section shapes reported in EN 10056-1 [34] in unlimited quantity. Even though an optimal design using new elements might have had a different layout (see Section 4.1.2), this way a consistent comparison and the quantification of environmental savings is possible [10].

Table 4 gives metrics for one transversal section with three central units and two end units. The structure made from reused elements (b) has 50% more mass with respect to the weight-optimized solution (a) which is made of elements of smaller cross sections, resulting in a better capacity utilization. However, the embodied energy and carbon of the structure made of reused elements are 63% and 56% lower respectively than those of the weight-optimized solution.

5. Conclusion

This paper presents structural optimization methods whereby structural layouts are obtained from a stock of reclaimed elements. Case studies show that the proposed optimization method produces optimal structures satisfying design criteria (ULS and SLS) in realistic scenarios. It is shown that even though structures made from reused elements have a higher mass and a lower element capacity utilization, they embody significantly less energy and carbon with respect to structures made of new elements. However, Life Cycle Assessment often contains many uncertainties and the energy and carbon impacts for instance associated with deconstruction processes might strongly vary. Future work could investigate the generality of these conclusions through more case studies. The two-step method presented in this paper, i.e. assignment and topology optimization followed by geometry optimization, might result in local optima. Future work could look into methods to search the solution space more efficiently, including simultaneous optimization of element assignment, topology and geometry.

Acknowledgements

The authors would like to thank *Swissgrid* AG for providing information useful to carry out the train station roof case study discussed in this paper and for granting permission to publish their records.

References

[1] European Environment Agency. Material resources and waste - the European environment - state and outlook. Luxembourg: Publications Office of the European Union; 2010.
[2] Allwood JM, Cullen JM. Sustainable materials - with both eyes open. Cambridge: UIT Cambridge; 2012.
[3] EUROSTAT. Waste statistics online database Available from: https://ec.europa.eu/eurostat/statistics-explained/index.php?title=Waste_statistics#Total_waste_generation; October 2017, Accessed date: 9 September 2018 [Online].
[4] Sartori I, Hestnes AG. Energy use in the life cycle of conventional and low-energy buildings: a review article. Energ Buildings 2007;39(3):249–57.
[5] Kaethner S, Burridge J. Embodied CO_2 of structural frames. Struct Eng 2012;90(5):33–40.
[6] Stahel WR. Policy for material efficiency - sustainable taxation as a departure from the throwaway society. Phil Trans R Soc A 2013(371).
[7] Iacovidou E, Purnell P. Mining the physical infrastructure: opportunities, barriers and interventions in promoting structural component reuse. Sci Total Environ 2016;557–558:791–807.
[8] Fujita M, Iwata M. Reuse system of building steel structures. Struct Infrastruct Eng 2008;4(3):207–20.
[9] Addis B. Building with reclaimed components and materials. London: Earthscan; 2006.
[10] Pongiglione M, Calderini C. Material savings through structural steel reuse: a case study in Genoa. Resour Conserv Recycl 2014;86:87–92.
[11] Yeung J, Walbridge S, Haas C, Saari R. Understanding the total life cycle cost implications of reusing structural steel. Environ Syst Decis 2017;37:101–20.
[12] Dunant CF, Drewniok MP, Sansom M, Corbey S, Cullen JM, Allwood JM. Options to make steel reuse profitable: an analysis of cost and risk distribution across the UK construction value chain. Clean Prod 2018;183:102–11.
[13] Gorgolewski M. Designing with reused building components: some challenges. Build Res Inf 2008;36(2):175–88.
[14] Brütting J, Senatore G, Fivet C. Optimization formulations for the design of low embodied energy structures made from reused elements. Advanced computing strategies for engineering. Springer; 2018.
[15] Rozvany G. Aims, problems and methods of structural optimization. Shape and layout optimization of structural systems and optimality criteria methods. Wien, New York: Springer; 1992. p. 1–5.
[16] Dorn WS, Gomory RE, Greenberg HJ. Automatic design of optimal structures. J Mec 1964;3:25–52.
[17] Achtziger W. On simultaneous optimization of truss geometry and topology. Struct Multidiscip Optim 2007;4:285–304.
[18] He L, Gilbert M. Rationalization of trusses generated via layout optimization. Struct Multidiscip Optim 2015;52(4):677–94.
[19] Toakley A. Optimum design using available sections. J Struct Div 1968;2:1219–41.
[20] Ghattas ON, Grossmann IE. MINLP and MILP strategies for discrete sizing structural optimization problems. Electronic computation. 1991. [Indianapolis].
[21] Rasmussen M, Stolpe M. Global optimization of discrete truss topology design problems using a parallel cut-and-branch method. Comput Struct 2008;86(13–14):1527–38.
[22] Nemhauser GL, Wolsey LA. Integer and combinatorial optimization. New York: Wiley; 1988.
[23] Fujitani Y, Fujii D. Optimum structural design of steel plane frame under the limited stocks of members. 2000.
[24] Bukauskas A, Shepherd P, Walker P, Sharma B, Bregula J. Form-fitting strategies for diversity-tolerant design. 2017.
[25] Haftka RT. Simultaneous analysis and design. AIAA J 1985;23(7):1099–103.
[26] Arora JS, Wang Q. Review of formulations for structural and mechanical system. Struct Multidiscip Optim 2005;30:251–72.
[27] Mela K. Resolving issues with member buckling in truss topology optimization using a mixed variable approach. Struct Multidiscip Optim 2014;50:1037–49.
[28] The Athena Sustainable Materials Institute. Demolition energy analysis of office building strcutural systems. 1997. [Ottawa].
[29] German Federal Ministry of the Interior, Building and Community. Ökobaudat - database for the life cycle assessment of buildings. 2017.
[30] European Standard EN 10220. Seamless and welded steel tubes - dimensions. 2002.
[31] Swiss Standard SIA 263:2013. Steel structures. 2013.
[32] Swiss Standard SIA 260:2003. Basis of structural design. 2003.
[33] Swiss Standard SIA 261:2014. Actions on structures. 2014.
[34] European Standard EN 11056-1. Structural steel equal and unequal leg angles - dimensions. 2017.